

Measurements of Plasma Potential Distribution in Segmented Electrode Hall Thruster

Y. Raitses, D. Staack and N. J. Fisch

Princeton University Plasma Physics Laboratory
P. O. Box 451, Princeton, NJ 08543

Abstract

Use of a segmented electrode placed at the Hall thruster exit can substantially reduce the voltage potential drop in the fringing magnetic field outside the thruster channel. In this paper we investigate the dependence of this effect on thruster operating conditions and segmented electrode configuration. A fast movable emissive probe is used to measure plasma potential in a 1 kW laboratory Hall thruster with segmented electrodes made of a graphite material. Relatively small probe-induced perturbations of the thruster discharge in the vicinity of the thruster exit allow a reasonable comparison of the measured results for different thruster configurations. It is shown that the plasma potential distribution is almost not sensitive to changes of the electrode potential, but depends on the magnetic field distribution and the electrode placement.

Introduction

Plasma-wall interaction plays an important role in operation of Hall thrusters. Several theoretical works predicted that the physical properties of the channel wall material, namely secondary electron emission and conductivity can strongly affect the electron temperature, electron mobility and, as a result, the whole structure of the acceleration and ionization regions [1-5]. Experimental studies of this effect were mainly implemented by a simple exchange of the channel wall material, for example, from ceramic to metal [2, 3, 6] or for different ceramics [7,8]. In addition, they were usually limited by measurements of integral discharge characteristics, which were, however, strongly

influenced by the channel material. For example, at the same operating conditions, an average ion velocity and discharge current were larger in the channel with a stainless steel walls than for a channel made from a boron nitride ceramic [6]. Thus, thruster performance might not be affected in the metal wall case. Some direct indications of the effect of secondary electron emission on the electron mobility was reported in ref. [3]. A larger electron temperature measured in the channel with metal walls was attributed to a lower secondary electron emission of this material.

As an alternative to the conventional use of a channel made from either ceramic or metal, a segmented electrode Hall thruster, which was suggested and studied in refs. [9-12] uses low emissive electrodes placed along a ceramic channel in order to control the electric field. In our previous studies we used segmented electrodes made from a LaB₆ material plated on a molybdenum ring [10] The results obtained with these electrodes demonstrated a plume reduction of about 20% compared to a conventional non-segmented thruster configuration [10,11]. In order to avoid a conductive coating of ceramic channel walls caused by sputtering of LaB₆, a segmented electrode made from a carbon-carbon-fiber material has been developed and used in a recent set of experiments. Measurements of plasma potential distribution indicated that the plume reduction effect is accompanied with a substantially smaller fraction of the voltage potential drop established in the defocusing fringing magnetic field of the segmented electrode thruster. [13]. Note that in this set of experiments, we achieved only 10 % of the plume reduction compared to a conventional configuration. In addition, the discharge current and the current collected by this electrode were significantly smaller. It was suggested that the

“Copyright © 2001 by Y. Raitses. Published by the Electric Rocket Propulsion Society with permission.”

observed differences between two sets of experiments may be attributed to differences in the magnetic field distribution, which was, for example, kept constant and not optimized in experiments with the graphite segmented electrode [13]. Moreover, the absence of a conductive coating on the outer channel wall could affect radial gradients of the electron pressure [14] leading to a degradation of the plume characteristics.

In the present work, we describe results obtained for segmented thruster configurations with single and two segmented electrodes placed on inner and outer channel walls and for two different magnetic field distributions. A relevance of these new results to the observed differences of plume characteristics in our previous experiments is suggested. Since a fast emissive probe is the key diagnostic tool of this work, some preliminary characterization of probe-induced perturbations of the plasma in Hall thruster is also presented.

Experimental Setup

Fig. 1 shows a 9 cm laboratory thruster with a single 4 mm length graphite segmented electrode placed on the inner channel wall near the thruster exit. The magnetic field distribution in the thruster channel is produced by two electromagnet coils, which are supplied from two separate power supplies. Simulated results for two different magnetic field distributions with different ratios of the internal coil current to the external coil current are shown in Fig. 2. Measurements of the magnetic field exhibited a good agreement with the results of non-linear simulations.

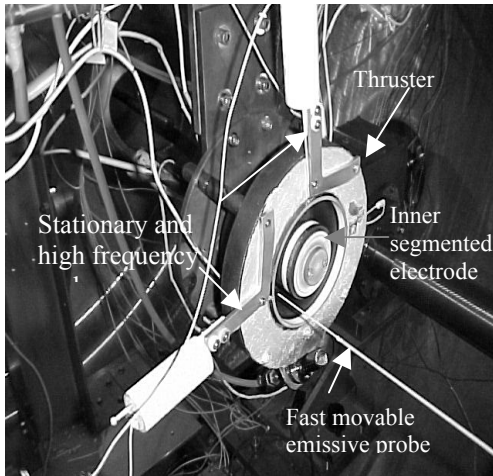


Fig. 1 Segmented electrode Hall thruster and probe setup.

The placement of the inner segmented electrode relative to the magnetic field distribution is shown in Fig. 2a. An additional graphite segmented electrode is placed on the outer wall as it shown in Fig. 2b. This 8 mm length electrode serves as the equivalent to a conductive coating, which was typically observed in experiments with LaB₆ electrodes as a result of their sputtering by ion bombardment [10-11].

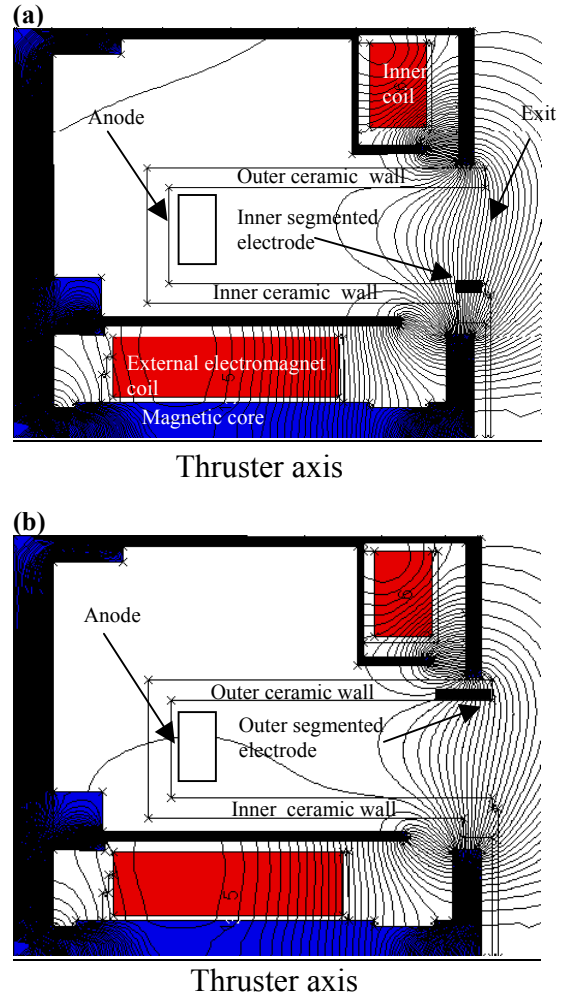


Fig. 2 Non linear simulations of the magnetic field distribution for two ratios of the internal to external coils currents: 2.1(a) and 5 (b). In addition, there is shown the placement of the inner (a) and outer (b) segmented electrodes in the channel

A fast movable emissive probe setup is used to measure plasma potential distribution (See Fig.1). The probe is made a 0.25 mm W-Th wire with a filament tip of etched to 0.1 mm diameter and loop length of about 2 mm. The wire is

inserted in alumina tube of about 1.2 mm. The positioning system provides a fast probe immersion in the axial direction from the distance of 20 cm of the thruster exit with a maximum speed of 500 mm/sec. In addition, it can maintain various positions of the probe in the radial direction relative to the thruster axis. Control of this positioning system and measurements of probe heating power and probe potential relative to the ground are performed by a PC-based data acquisition system. Other measurements included mass flow rate, discharge current and voltage, electromagnetic coils current, potential of the floating segmented electrode relative to the ground and current to the cathode biased electrode. Also the angular ion flux distribution was measured by a movable flat Langmuir probe with a guarding sleeve [13]. The thruster, test facility and probe setup used in this study have been described in greater details in refs. [9-11,13].

Experimental results

The measurements of the plasma potential were conducted for two segmented electrode configurations: 1) single segmented with the electrode placed only on the inner wall; 2) two segmented, with an additional outer electrode placed on the outer wall. Through all these measurements the thruster operated at the same discharge voltage of 250 V, xenon gas flow rate of 1.7 mg/s for the anode and 0.3 mg/s for the cathode. The inner segmented electrode was either floating or cathode biased, while the outer electrode was always under floating potential. The effect of the magnetic field distribution was measured for two coils current ratios of 2.1 and 5 (Fig. 2).

The procedure of emissive probe measurements is described in details in ref. [13]. The emissive probe was operated in a strong electron emission regime, which was typically achieved at 30 W of the heating power from an external power supply. In general, reproducibility of probe measurements in the present set of experiments was more than 85%. The major source of irreproducibility was probe-induced perturbations of the thruster discharge causing an increase of the discharge current as the probe moved towards the anode. Typical traces of the discharge current versus the probe position along the mid line of the channel are shown in Fig. 3. As can be seen, the behavior of the discharge

current during the probe immersion can be affected by probe construction and material, heating power and channel wall material. Similar amplitudes of the discharge current measured for hot emissive and cold probes indicate that surface temperature of the probe tube has insignificant affect on perturbations. On the other hand, the electrons emitted by the hot probe may couple with plasma in a way that the discharge current increases more rapidly than the cold probe in the vicinity of the thruster exit (See Fig. 3). In the absence of the filament wire, perturbations caused by the immersion of the alumina tube still persist, but with substantially smaller amplitudes than with the filament. Thus, ablation of the probe tube heated by the plasma [15] is not a sole cause of these perturbations.

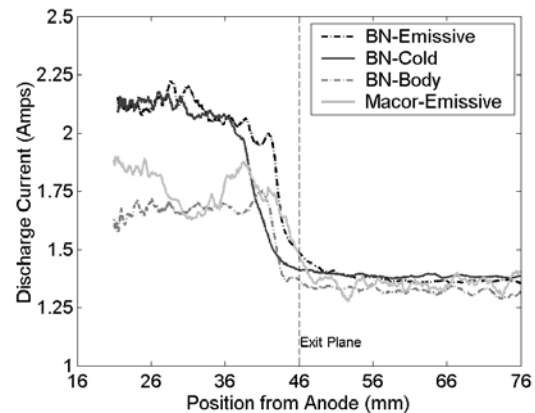


Fig. 3 Probe induced perturbations of the discharge current measured at the same operating conditions, 250 V and 1.7 mg/s for non segmented thruster: hot emissive probe, cold probe and alumina tube without a probe filament (body); and for the thruster with a ceramic spacer made from MACOR material.

Interestingly, although we did not observed considerable differences in probe-induced perturbations for the segmented and non-segmented thruster configurations, a replacement of the inner segmented electrode by a ring-shaped spacer made from MACOR ceramic material resulted in a significantly reduction of their amplitude even for the hot probe (See Fig. 3). This result may be an indication that the observed discharge current perturbations are originated from an interaction of plasma with channel and probe walls and therefore, affect plasma properties in the entire channel.

Uncertainties caused by probe-induced perturbations make difficult comparison of the plasma potential distribution measured for different thruster configurations and operating regimes. The electric field derived from such perturbed measurements can exceed typical values obtained for conventional Hall thrusters [15,16]. As an example, Fig. 4 shows counter plots of equipotentials measured with different amplitudes of perturbations for the non-segmented thruster and for the thruster with a MACOR spacer. A sharp increase of the density of counter lines, i.e, the electric field, in the non-segmented case than in the thruster configuration with the spacer can be attributed either to differences in probe induced perturbations or to differences in the physical properties of MACOR and boron nitride ceramics. In order to smooth such uncertainties of the measured plasma potential distribution for different segmented thruster configurations, the following analysis is mainly focused on the results obtained in the vicinity of the thruster exit and outside the channel, in which perturbations are relatively small.

Tables 1 lists discharge current, segmented electrode current/floating potential and plume angle measured for single segmented and two segmented configurations of the thruster with two different magnetic field distributions shown in Fig. 2.

Table 1: Integral thruster parameters for segmented and non-segmented thruster configurations: discharge current, I_d , current to segmented cathode biased electrode I_{seg} , floating potential of the segmented electrode relative to the cathode, V_f , Plume angle estimated for 90% of the total ion flux from the thruster.

Thruster Configurations	I_d A	I_{seg} mA	V_f V	Plume Angle Deg
Non-segmented	1.57	-	-	100
One segmented Fig. 2a	1.61	-	22	90
	1.65	56	-	87
Two segmented Biased	1.70	70	-	82(min)
One segmented Fig. 2b Floating	1.67	-	12.5	100

The plasma potential distribution measured for these configurations are shown in Figs. 5 and 6.

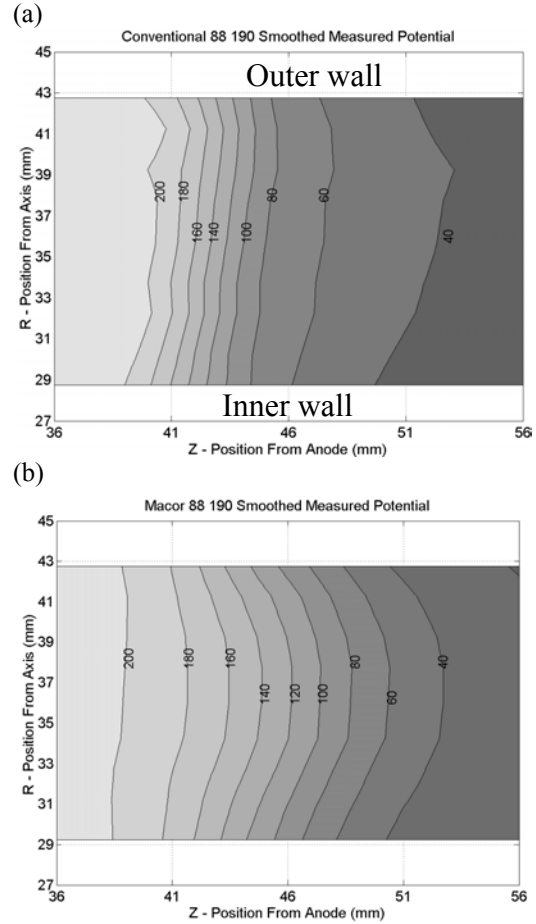


Fig. 4 Plasma potential distribution measured for the non-segmented thruster and for the thruster with a MACOR spacer placed on the inner wall at the thruster exit. The channel length from the anode to the exit is 46 mm. The channel height is 18 mm.

In general, the acceleration region in the all segmented electrode configurations is more inward than in the conventional non-segmented case (Fig. 4). Therefore, a fraction of the voltage drop established outside the channel in the defocusing fringing magnetic field is smaller for the segmented configurations than in the non-segmented case. These results, which can be partially attributed to a lower secondary electron emission of the graphite electrodes than the ceramic channel, are in a qualitative agreement with theoretical predictions of ref. [14]. In addition, an ion collector role of the segmented electrode can also contribute to a reduction of the plasma potential at the thruster exit.

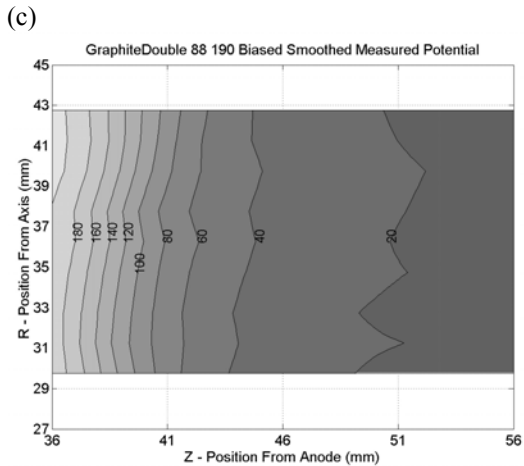
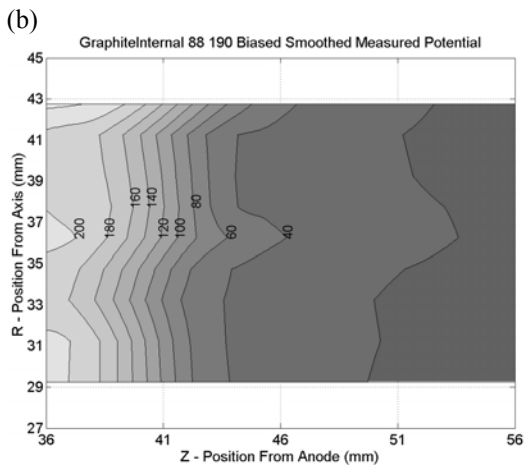
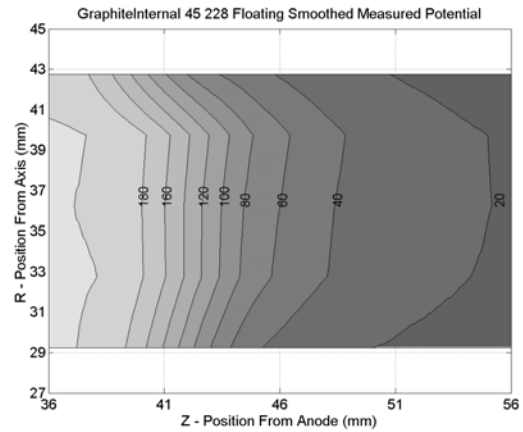
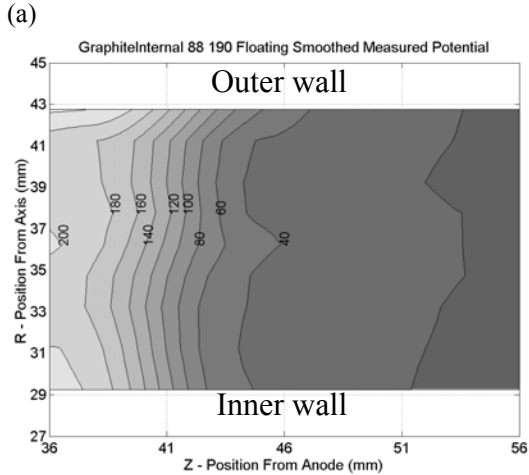


Fig. 5 Plasma potential distribution measure for the single segmented, floating (a) and biased (b) and double segmented with the inner electrode biased (c) configurations. The thruster was operated with the magnetic field distribution shown in Fig. 2a. The channel exit is 46 mm from the anode.

Fig. 6 Plasma potential distribution measured for the single segmented electrode configuration of the thruster with the magnetic field distribution shown in Fig. 2b. The channel exit is 46 mm from the anode.

The bias applied to the segmented electrode almost does not change the plasma potential distribution. Similar to a simple electrostatic probe, the electrode collects the same flux of ions arriving probably from the same region of the plasma. Assuming that collected ions reach Bohm's velocity at the sheath-presheath interface can be roughly estimated from the measured current to the biased segmented electrode. For example, for the electron temperature of 10 eV, this density is $\sim 2 \cdot 10^{17} \text{ m}^{-3}$. As could be expected this figure is smaller than measured in conventional thruster without segmented electrodes and therefore, with a large electric field outside the thruster channel [16].

In the case of the single segmented electrode configuration the opposite outer wall is made of a boron nitride ceramic with a higher secondary electron emission than graphite at the same energy of primary electrons. Following theoretical model of ref. [14], this difference can affect a radial temperature gradient and, as a result, the concave shape of equipotentials similar to the measured results of Fig. 5. These predictions are also supported by the results obtained for the thruster with two-segmented electrode made of the same material and placed on the outer and inner walls at the exit. In this thruster case, the measured plasma potential changes insignificant in the radial direction. In addition, a larger current to the inner segmented

electrode was measured than for the single segmented configuration (Table 1).

Remarkably, of all thruster configurations used in these experiments, the plume angle measured in the two-segmented case is narrowest. Furthermore, it is just a few degrees larger than the result reported in ref [10,11]. Thus, metal coating of the outer ceramic wall in our previous experiments with the single inner segmented electrode made of LaB₆ played indeed a crucial role affecting the shape of equipotentials and, as a result, the plume angle reduction.

Finally, a comparison of the results shown in Figs. 5 and 6 for the single segmented electrode configuration suggests that the magnetic field distribution can also strongly affect equipotentials and, as a result, the plume angle. The shape of equipotentials is changed from the focusing concave to the defocusing convex for Figs. 2a and 2b respectively. In a different set of experiments, the magnetic field distribution of Fig.2b was also applied for the non-segmented thruster configuration. However, probe measurements were difficult to implement because of unstable thruster operation in this regime.

Summary & Conclusions

Measurements of the plasma potential distribution in Hall thruster revealed the possibility of control of placement of the acceleration region in the thruster channel by the non emissive electrodes placed on the inner and outer walls at the thruster exit. In fact, the electric field established outside the thruster channel in the fringing magnetic field was twice smaller than for the conventional non-segmented thruster configurations. The shape of equipotentials in Hall thrusters depends strongly on physical properties of the channel materials, in particular, at intersections of the magnetic field lines with the outer and inner channel walls. It is suggested that the overall effect of the segmented electrodes is due to a secondary electron emission and ion collector role of the electrodes.

In the case of the two segmented electrode configurations, the plasma potential is almost not changed in the radial direction and the plume reduction of 18% was achieved. This result demonstrated that in our previous experiments with a single LaB₆ electrode placed on the inner wall, the metal coating of the outer ceramic wall

caused by sputtering of this electrode played an essential role in obtaining similar plume reduction effect.

Interestingly that a reduction of the fraction of the voltage potential drop outside the channel and control of the shape of equipotentials in the two segmented electrode case led only to a 18 deg plume angle reduction as compared to the non-segmented thruster with 100 deg a plume angle. Thus, in addition to the defocusing fringing magnetic field and radial gradients of the electron pressure in the channel, there are other stronger mechanisms causing a large plume angle in Hall thrusters. Perhaps, some of these mechanisms can be still controlled through a precise placement of segmented electrodes in the channel and magnetic field distribution.

Acknowledgment

The authors benefited from many discussions on the effect of segmented electrodes with Dr. Michael Keidar and Prof. Amnon Fruchtman. The authors would like to thank Mr. L. A. Dorf and Mr. A. A. Litvak for their help in experiments and in preparation of this paper.

This work was supported by grants from New Jersey State Science and Technology Commission and by the US Department of Energy under Contract No. DE-AC02-76CHO3073.

References

1. A. I. Morozov and V. V. Savelyev, in *Review of Plasma Physics*, edited by B.B. Kadomtsev and V. D. Shafranov, Consultants Bureau, New York, 2000, Vol. 21, p. 203.
2. V. V. Egorov, V. Kim, A. A. Semenov and I. I. Shkarban, in *Ion Injectors and Plasma Accelerators*, Energoizdat, Moscow, 1990, p. 56 [in Russian]
3. G. E. Bugrov, V. A. Ermolenko and V. K. Charchevnikov, Formation of Electron Distribution Function in Hall Thrusters with Dielectric and Metal Walls, the 6th All-Union Conference on Plasma Accelerators and Ion Injectors, Dnepropetrovsk, 1986, pp 33-34 [in Russian]
4. M. Keidar, I. D. Boyd and I. I. Beilis, Plasma flow and plasma-wall transition in Hall thruster channel, submitted to *Phys. Plasmas*.
5. E. Y. Choueiri, AIAA paper 2001-3504, Salt Lake City, UT, July 2001.

6. S. A. Chartov, Effect of the channel material on integral characteristics of Hall thrusters, the 6th All-Union Conference on Plasma Accelerators and Ion Injectors, Dnepropetrovsk, 1986, pp 33-34 [in Russian]
7. J. B. Bugeat and C. Koppel, IEPC paper-95-35, the 24th IEPC conference, Moscow, 1995
8. Y. Raitses, J. Ashkenazy and G. Appelbaum, IEPC paper 97-056, the 25 IEPC conference, Cleveland, OH, 1997.
9. N. J. Fisch, Y. Raitses, L. A. Dorf and A. A. Litvak, Design and Operation of Hall Thruster with Segmented Electrode, AIAA paper 99-2572, Los Angeles, CA, June 1999.
10. Y. Raitses, L. A. Dorf, A. A. Litvak and N. J. Fisch, J. Appl. Phys. **88**, 1263, 2000.
11. N. Fisch, Y. Raitses, L. A. Dorf and A. A. Litvak, J. Appl. Phys. **89**, 2040, 2001.
12. A. Fruchtman, N. J. Fisch and Y. Raitses, Phys. Plasmas, **8**, 1048, 2001.
13. Y. Raitses, D. Staack, A. Smirnov, A. Litvak, T. Graves, L. Dorf and N. J. Fisch, AIAA paper 2001-3776, Salt Lake City, UT, 2001.
14. Y. Raitses, M. Keidar, D. Staack and N. J. Fisch, Effect of segmented electrodes on Hall thruster plasma, Submitted to Phys. Plasmas.
15. J. M. Haas and A. D. Gallimore, Rev. Sci. Instrum, **71**, 4131, 2000.
16. J. M. Haas and A. D. Gallimore, Phys. Plasmas, **8**, 652, 2001